# Calculations of Viscous Transonic Flow over Airfoils

Z. B. Chen* and P. Bradshaw†
*Imperial College, London, England*

**A simple and economic iterative scheme is presented for calculating compressible viscous boundary layers and wakes over airfoils and for matching the shear-layer calculations to the calculations of the transonic potential external flows. The iterative scheme is an extension and improvement of the scheme developed by Mahgoub and Bradshaw for calculating incompressible flow. A new iterative method in the shear-layer calculations has been designed and applied in the near-wake region. The computing time is only a little greater than in conventional displacement-surface calculations that ignore normal pressure gradients and consequently incur errors in the near wake. Some comparisons are made with full Navier-Stokes solutions and experimental data.**

## Introduction

CONSIDERABLE effort is currently being devoted to the solution of the full time-averaged Navier-Stokes equations, with appropriate turbulence model equation(s), using explicit time-dependent methods,[1] implicit factorization methods,[2] etc. However, the computing time is often too expensive for engineering purposes. It seems certain that methods involving separate calculations of the laminar and turbulent shear layers over airfoils and in the wake and of inviscid flow external to these layers, together with a matching process that enables the mutual interaction of these flows to be determined, will continue to have a practical advantage in both computing time and accuracy for a wide variety of engineering problems.

In this paper we will present an iterative scheme of this kind, which can be regarded as an extension and improvement of a scheme developed for incompressible flow.[3]

The conventional displacement-surface methods may be inaccurate on highly curved surfaces or in the wake near the trailing edge where streamline curvature is extremely high, since they ignore the normal pressure gradient that may have a significant effect on the solution.

With the new iterative method for the shear-layer calculations presented here, the effects of normal pressure gradient, even where they are relatively large and changing rapidly in the streamwise direction, can be included by iterative improvement of a marching calculation rather than by a fully elliptic calculation. Therefore, the whole iterative scheme remains simple and the cost of computing time is low. The pressure, but not the velocity, in the shear layer is stored from one iteration to the next: this means that only the pressure is allowed to transmit upstream influence, so that the method is nominally restricted to attached flow.

Jameson's potential flow calculation method[4-6] has been modified and applied in the present calculation of compressible flows external to the shear layers. It smears shock waves over at least two mesh widths, so discontinuities need not be included in the shear-layer calculation.

The compressible boundary-layer calculation method described in Ref. 7 has been extended to an $s$, $n$ coordinate system. A simple compressibility correction has been made to the incompressible wake program, in advance of a major upgrade of the compressible wake calculation.

Several sample calculations are compared with experimental data and other computational results.

Presented as Paper 82-0997 at the AIAA/ASME Third Joint Thermophysics, Fluids, Plasma and Heat Transfer Conference, St. Louis, Mo., June 7-11, 1982; submitted June 17, 1982; revision received April 25, 1983. 

*Academic Visitor, Department of Aeronautics (on leave from Chinese Aerodynamic Research and Development Center, Mian Yang, Sichuan, China).

†Professor, Department of Aeronautics.

## Analysis

### Shear-Layer Calculation

The time-averaged Navier-Stokes equations for a compressible gas with viscous and/or turbulent stress $\sigma_{ij} = \sigma_{ij}$ can be written for two-dimensional transonic flow as

$$U\frac{\partial U}{\partial x} + V\frac{\partial U}{\partial y} = -\frac{1}{\rho}\frac{\partial p}{\partial x} + \frac{1}{\rho}\left(\frac{\partial \sigma_{xx}}{\partial x} + \frac{\partial \sigma_{xy}}{\partial y}\right) \tag{1}$$

$$U\frac{\partial V}{\partial x} + V\frac{\partial V}{\partial y} = -\frac{1}{\rho}\frac{\partial p}{\partial x} + \frac{1}{\rho}\left(\frac{\partial \sigma_{xy}}{\partial x} + \frac{\partial \sigma_{yy}}{\partial y}\right) \tag{2}$$

$$U\frac{\partial T}{\partial x} + V\frac{\partial T}{\partial y} = \frac{U}{\rho c_p}\frac{\partial p}{\partial x} + \frac{\epsilon}{c_p} - \frac{1}{\rho}\left(\frac{\partial q_x}{\partial x} + \frac{\partial q_y}{\partial y}\right) \tag{3}$$

with the continuity equation

$$\frac{\partial \rho U}{\partial x} + \frac{\partial \rho V}{\partial y} = 0 \tag{4}$$

In the present calculations, we represent $\sigma_{xy}$ and the turbulent energy dissipation rate $\epsilon$ by Bradshaw's turbulence model equation.[7] Other Reynolds stresses are represented by empirical multiples of $\sigma_{xy}$, but the solution procedure could also be used with other turbulence model equation(s).

The shear-layer calculations are carried out in semi-curvilinear ($s$, $n$) coordinates, the $s$ axis being coincident with the (curved) surface; the $n$ coordinate lines (constant $s$ lines) are straight and normal to the $s$ axis. For simplicity, however, the description will be presented in $x$, $y$ coordinates. The shear-layer calculation is matched to the outer inviscid calculation at the nominal edge of the shear layer: displacement-thickness concepts are not used. After one marching calculation of the shear layer, the calculated velocity normal to the matching surface provides the inner boundary condition for an inviscid flow calculation, which in turn provides the tangential velocity or pressure as the outer boundary condition for another shear-layer calculation. So the boundary conditions for this elliptic system of equations for the shear layer [Eqs. (1-4) plus the turbulence model] are, for the boundary-layer case, as follows: at the real surface, $U=0$, $V=V_w$, and at the matching surface, $p=p_e(x)$. Starting from the stagnation point, we use a compressible version of Thwaites' method to calculate the laminar

boundary layer[8]: an empirical criterion is used to predict the transition position at which we use the method of Ref. 9 to create the initial profiles of velocity, Reynolds stress, and temperature for the turbulent flow calculation. For the wake calculation, the pressure $p=p_e(x)$ is specified at both upper and lower matching surfaces and the initial profiles in wake coordinates at the trailing edge are provided by interpolating the results of the boundary-layer calculation at the last two streamwise steps into a new $(s, n)$ coordinate system aligned with one edge of the wake.

For the potential flow calculation, the normal velocity is specified at the matching surface and the conditions at infinity are the same as in ordinary potential calculations. Some care has to be taken to represent the Kutta condition. In the present method, we carry on the wake calculation until, say $x=1.5c$, and impose what is nominally the Kutta condition at $x=1.5c$. Between $x=c$ and $1.5c$, we use the pressure difference across the wake, obtained from the wake calculation, to get the difference of potential $\Delta\phi$ across the wake. Therefore, between $x=c$ and $1.5c$, $\Delta\phi$ is a function of $x$, but after $x=1.5$, $\Delta\phi$ remains constant, i.e., no pressure difference, as in ordinary potential calculations. Clearly, the pressure difference across the wake must be negligible so far behind the airfoil, and this use of the Kutta condition is both weak and uncontroversial. At the trailing edge, we now assume that the (viscous) separation streamline has zero curvature, but this directly affects only the calculation within one mesh width from the trailing edge and is quite compatible with relatively large pressure difference across the wake.

Then, a shear-layer calculation "sweep" proceeds through both boundary layers and the wake, taking the pressures at the matching surfaces as known from the preceding inviscid calculation. The calculation loop for the shear layer is executed as follows:

1) On the first sweep, guess $p(x,y)$ for given $p_e(x)=p(x,y=\delta)$; in the present program we simply set $p(x,y)=p_e(x)$.

2a) Calculate the laminar boundary layer up to the transition point, neglecting $\partial p/\partial y$ on all sweeps.

2b) Calculate the $U$ and $\sigma$ stresses at the end of one streamwise step in the turbulent shear layer, with known $\partial p(x,y)/\partial x$, evaluated from $p(x,y)$ by central differences in $x$ in the region where $\partial^2 p/\partial x\partial y$ varies significantly with $y$.

3) Calculate $V$ at the end of the step from the ordinary differential equation in $y$ (along the normal characteristic) that results from substituting Eq. (4) into Eq. (1) when $U$, $p$, and $\sigma$ stresses are known at all $y$.

4) Calculate $p$ at the end of the step by integrating Eq. (2) with boundary value(s) of $p$.

5) With new $p$, recalculate $V$ at the same step as in step 3.

6) Repeat steps 4 and 5 until variations of $V$ are small enough.

7) Using $V$ and $p$ from steps 4 and 5, recalculate $U$ and $\sigma$ stresses, i.e., repeat step 2b.

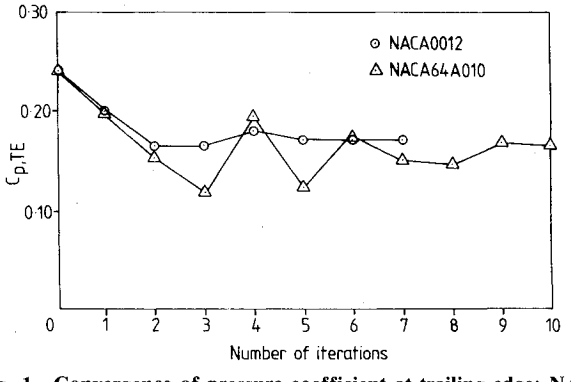


**Fig. 1 Convergence of pressure coefficient at trailing edge: NACA 0012 at $M_\infty=0.8$, $\alpha=0$, $U_\infty c/\nu_\infty=3.5\times10^6$; NACA 64A010 at $M_\infty=0.8$, $\alpha=0$, $U_\infty c/\nu_\infty=2.0\times10^6$.**

8) Repeat steps 2b-7 several times. In the present calculation, we do this only twice: as explained below, iteration to convergence is not needed since it is merely an aid to stability in the early sweeps.

9) With $U$, $V$, $\tau$, and $p$ now known, calculate $T$ by the method of Ref. 7 (i.e., assuming a constant turbulent Prandtl number).

10) Repeat steps 2b-9 for the next shear-layer step, until $x=1.5c$. If necessary, change the matching surface to lie just outside the edge of the recalculated shear layer.

11) Repeat steps 2-9 with new pressure distributions at the matching surfaces by recalculation of potential flow.

When $\partial^2 p/\partial x\partial y$ is small, we can omit steps 5-8 and the iterative method is the same as in Ref. 3.

Because $p$ varies quite smoothly with $y$ (at least when shock waves are smeared out by the inviscid flow calculation, we represent $p(x,y)$ as a fifth-order polynomial of $y$ at each streamwise station $x$, i.e.,

$$p(x_i,y)=a_5(x_i)(y/\delta)^5+a_4(x_i)(y/\delta)^4+a_3(x_i)(y/\delta)^3+a_2(x_i)(y/\delta)^2+a_1(x_i)(y/\delta)+a_0(x_i) \quad (5)$$

Coefficients for this polynomial are obtained by fitting a polynomial to $\partial p/\partial y$ values evaluated directly from Eq. (2) at five finite difference mesh points: step 4 is simply an analytic integration of the polynomial $\partial p/\partial y$. Thus, the pressure need not be stored at each mesh point: we store only the coefficients $a_j(x_i)$ in Eq. (5) as a two-dimensional array $6\times M$

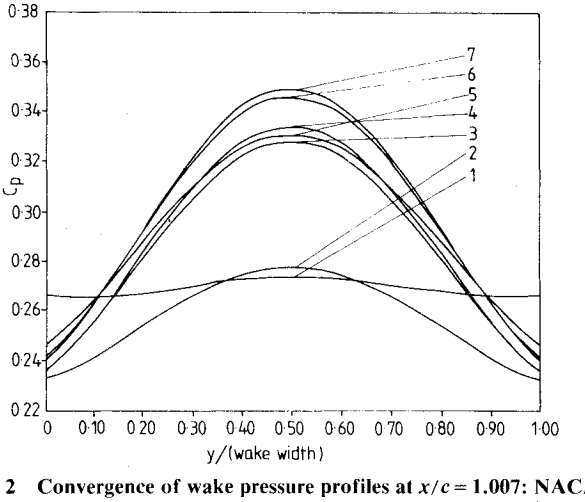


**Fig. 2 Convergence of wake pressure profiles at $x/c=1.007$: NACA 0012, conditions as in Fig. 1.**

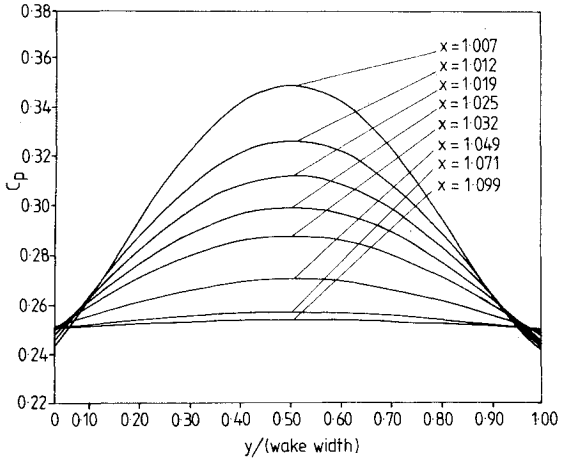


**Fig. 3 Wake pressure profiles for $1.007<x/c<1.099$: NACA 0012, conditions as in Fig. 1.**

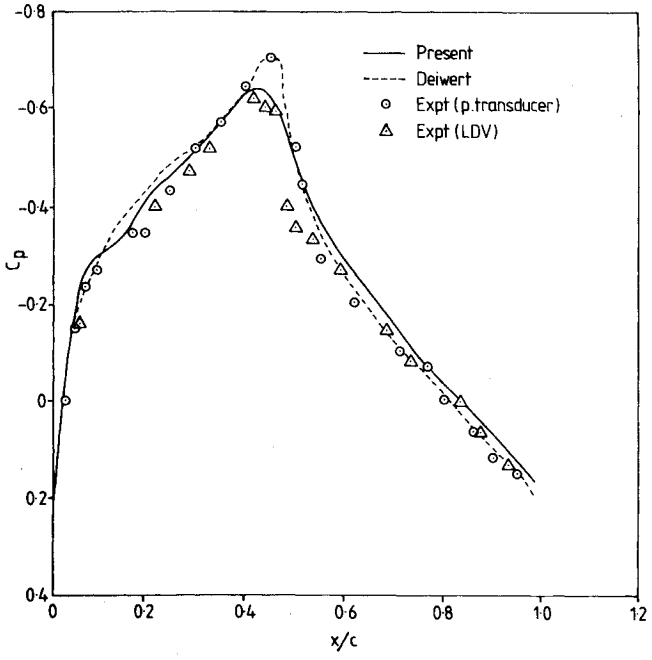


**Fig. 4 Comparison of experiment,[12] present calculations and Navier-Stokes calculations: pressure distribution for NACA 64A010 at $M_\infty = 0.8$, $\alpha = 0$, $U_\infty c/\nu_\infty = 2.0 \times 10^6$.**

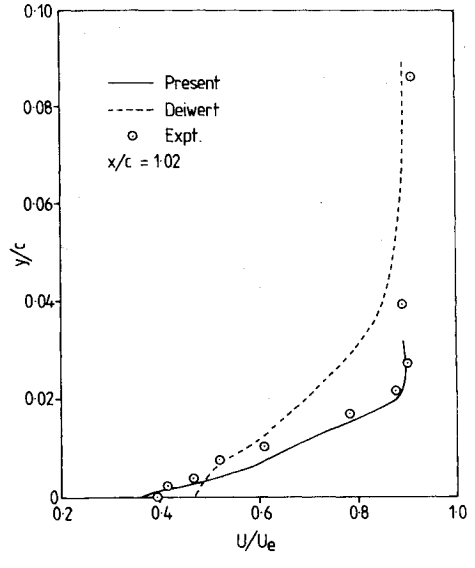


**Fig. 5 Comparison of experiment and calculation for near-wake velocity profile: details as in Fig. 4.**

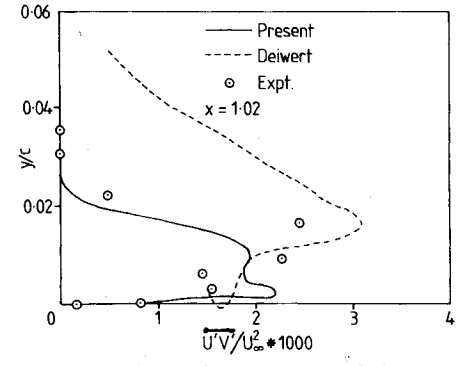


**Fig. 6 Comparison of experiment and calculation for near-wake shear-stress profile: details as in Fig. 4.**

where $M$ is the total number of $x$ steps in regions of significant $\partial p/\partial y$.

In steps 2 and 3, the method of characteristics developed by Bradshaw et al.[7] is used. In the wake calculations, Bradshaw's interactive hypothesis[10] is used to treat the wake as two boundary layers that "time share" in the interactive region.

As mentioned before, when $\partial^2 p/\partial x \partial y$ is not large, we can omit steps 5-8 and represent $\partial p/\partial x$ by central difference. Because the pressure at adjacent streamwise stations is coupled via the inviscid flow calculation, this scheme is adequately stable, providing the upstream influence due to $x$-wise stress gradients is small. Indeed, we found that even when the upstream influence of $x$-wise stress gradients is relatively large, say in the region where the shock waves appear, this scheme is still stable. But when values of $\partial^2 p/\partial x \partial y$ are relatively high, the marching iterative method, in which the pressure field calculated on the last sweep is used for $\partial p/\partial x$, may fail. The reason is presumably that, if $\partial p/\partial x$ is changing rapidly with $x$, $\partial p/\partial y$ at given $x$ will depend rather strongly on the previous history of the shear layer, specifically the external pressure distribution. Since the external pressure distribution changes from sweep to sweep, the $p(y)$ profile calculated on, say, the $N$th sweep and used for the $U$, $V$, $\tau$ calculation on the $N+1$th sweep may be markedly different, when $N$ is small, from the actual $p(y)$ profile corresponding to the current external pressure distribution and the newly calculated $U$, $V$, $\tau$. Note that $p(y)$ is a special case because only $p(y)$ is stored from one sweep to the next; this mechanism of instability does not arise for the other variables.

A possible, but expensive, cure is to use a complete elliptic iterative method (e.g., Ref. 11). In the present work, we use a local iterative scheme in the shear-layer calculation, represented by the repetitions of steps 2b-7, using the new pressure at each point as soon as it has been calculated. The describing of $\partial p/\partial x$ by forward differences in $x$ can represent the upstream influence of pressure disturbance more accurately, so as to make the solution of each streamwise step closer to the real solution with the given boundary conditions for that sweep. (Since instability due to sweep-to-sweep changes in $p_e$ is a serious possibility only in the early sweeps, there is no point in repeating steps 2b-7 to convergence.) This "Gauss-Seidel" strategy implies that $\partial p/\partial x$ at a given point is obtained from the difference of an "old" downstream pressure and a "new" upstream pressure; however, this appears to have no ill effects, whether the pressure is increasing or decreasing from one sweep to the next.

As stated before, the shear-layer calculations with given edge pressure $p_e(x)$ yield values of $V_e(x)$ at the matching surface and the pressure difference across the wake. Then, the potential flow outside the matching surface can be calculated again and the process repeated to convergence.

### Inviscid Calculation and Matching Iteration

Some modifications have been made to Jameson's method, including provision of nonzero normal velocity boundary condition, a different treatment of Kutta condition as described above, and, a specially designed polynomial function added to the original coordinate transformation functions to cluster more mesh points near the trailing edge.

The complete calculation process is nearly the same as Ref. 3:

1) Guess the position of the matching surface, guess $V_e(x)$, and solve for the potential flow outside the matching surface to get $p_e(x)$ on the matching surface.

2) Execute steps 1-9, that is, one sweep of shear-layer calculation inside the matching surface, and then modify the position of matching surface according to the thickness of the shear layers if necessary (not necessary in the late stages of convergence).

3) Solve the potential flow with new $V_e(x)$ and get new $p_e(x)$. Deduce new values of $p(x,y)$ inside the matching

surface by assuming that $\partial p/\partial y$ remains the same as that calculated in step 2.

4) Repeat steps 2 and 3 until convergence is achieved.

Some care is needed in the discrete representation of $p_e$ and $V_e$, because the inviscid and shear-layer solutions depend on them and their streamwise derivatives. Some smoothing of the calculated values is advisable, especially near the trailing edge. For example, in the early stages of convergence separation may occur near the trailing edge, so some smoothing of the calculated pressure is needed to make the shear-layer calculation feasible. This kind of smoothing is *not* needed in the later stage of convergence, does not affect the final solution, and can therefore be applied informally where needed.

A sweep-to-sweep under-relaxation factor of 0.3 is applied only to the values of pressure inside the matching surface. No attempt has yet been made to optimize this relaxation factor, but for samples we calculated, only 10 or less sweeps are needed for convergence, starting from the very crude guess $\partial p/\partial y=0$ in the shear layers. From Fig. 1, we can see the convergence of pressure at the trailing edge, which is a most sensitive indicator of convergence. It converges very quickly, but nonmonotonically. From Fig. 2, we can see the convergence of the pressure distribution across the wake at the first calculation station downstream of the trailing edge, where the values of $\partial p/\partial y$ normally are very high and changing somewhat rapidly as iteration proceeds; however, they converge very fast and monotonically. These interesting facts demonstrate the fast convergence characteristics of the present scheme. If we attempt to reduce the number of iterative sweeps, Fig. 1 suggests that we may decrease the relaxation factor and Fig. 2 suggests an increase in relaxation factor. So no large improvement can be expected unless different values of the relaxation factor are used in different regions.

Only a little more computing time, spent in the calculation of $\partial p/\partial y$ and in "housekeeping" operations, is needed than in the conventional matching method using a displacement thickness. For one sweep of viscous/inviscid calculations, consisting of 115 streamwise stations with 25 points across the shear layer in the calculation of the boundary layers, 30 streamwise stations and about 45 points across the shear layer in the wake calculation, and $80\times20$ mesh points in the potential calculations takes about 230 s on CDC 6500 about half of which is used in the potential flow calculation.

The maximum amount of core needed is less than 26,000 decimal words, the core being arranged to overlay the separate programs for the viscous and inviscid calculations.

## Results

Sample calculations are shown in Figs. 1-7. Figures 1 and 2 show the convergence of calculations for an NACA 0012 airfoil at $M_\infty=0.8$, $\alpha=0$ deg, $Re=3.5\times10^6(U_\infty c/\nu)$ as discussed before. Figure 3 shows the pressure distribution in the wake for the same conditions. Near the trailing edge, we can see that both $\partial p/\partial y$ and $\partial/\partial x(\partial p/\partial y)$ are quite large. The pressure coefficient at the center of the wake reaches nearly 1.5 times the value of the pressure coefficient at its edge. At $x=1.1c$, $\partial p/\partial y$ is already negligible.

Figures 4-6 show the results for an NACA 64A010 airfoil with the same conditions as those in the experiments of Ref. 12, i.e., $M=0.80$, $\alpha=0$ deg, $Re=2\times10^6(U_\infty c/\nu)$, and transition position at $x=0.17c$.

Figure 4 shows the pressure distribution over the airfoil surface. The two sets of data were obtained in the same conditions but using different measuring techniques, one using a pressure transducer and the other the laser technique. The agreement between the present results and the experimental data or full Navier-Stokes solutions[12] is fairly good. The full Navier-Stokes solutions were obtained by Deiwert's method.

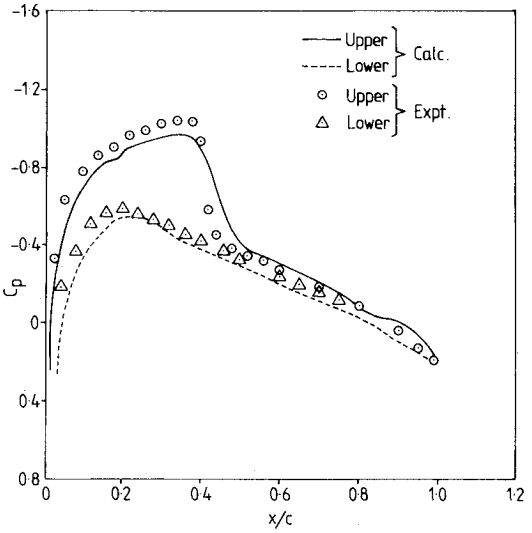


**Fig. 7 Comparison of experiment[13] and present calculation: pressure distribution for NACA 0012 at $M_\infty=0.775$, $\alpha=1$ deg, $U_\infty x/\nu=3.5\times10^6$.**

The present results have a slightly lower maximum $c_p$ value and the shock wave position is about 2% of chord further forward than in the experiment. Some error is probably caused by the rather small number of mesh points in the potential calculation. Figure 5 shows the velocity profile in the wake. The present results are much better than the complete Navier-Stokes solution, which had too coarse a mesh in the shear layer, and in good agreement with experimental results. Figure 6 shows the velocity correlation across the wake. The trend is similar to the experimental results. The thickness of the wake is nearly the same as the experimental data, but the full Navier-Stokes result is nearly two times in error: as is clear from Ref. 12, the shear-layer mesh was very coarse. Figure 7 shows the result of an asymmetrical case. This is for an NACA 0012 airfoil with the same conditions as in Ref. 13, except the transition position. In the present calculation $x_T=0.166c$ (because of the limit in the maximum size of the arrays in the shear-layer calculations), but in the experiment $x_T=0.05c$. The calculated result shows lower pressure values on both surfaces, but the discrepancy is not large. It should be noted that no corrections for blockage and lift interference were made to the experimental data.

It is noted that there are significant variations of the pressure in the near-wake region in both the $s$ and $n$ directions. From this we see that classic boundary theory, in which the normal pressure gradient is ignored, is questionable or clearly inaccurate in the near-wake calculation. It is not clear whether or not higher-order boundary-layer methods, such as those adopted in the Lock[14] and LeBalleur[15] transonic viscous/inviscid interaction calculations, could include the effect of the normal pressure gradient adequately. However, in the present method, the accuracy of the shear-layer calculation including the near-wake calculations should be comparable to Navier-Stokes solutions; thus, the accuracy of the viscous transonic flow calculation should be better than that of other methods based on various boundary-layer approximations for a given inviscid flow calculation method.

## Conclusions

The procedure just described is economical in time and storage and avoids all of the difficulties of breakdown of the boundary-layer approximation near the trailing edge or in other regions of large streamline curvature. It can be applied in the calculations of transonic or subsonic flow, attached or with minor recirculation, for engineering purposes.

The accuracy of the present procedure should be as good as that of full Navier-Stokes solutions using the same mesh and

turbulence model, but the partitioning of the flow into viscous and inviscid regions leads to a much more efficient solution and to convergence in only about 10 major iterations.

## Acknowledgments

This work was associated with a research agreement with the Ministry of Defence (PE). The authors are grateful to Dr. I. Kullar, Dr. M. A. Kavanagh, Dr. H. E. Mahgoub, and Mr. D. Mobbs for details of their incompressible flow calculations, which were the preparatory work for the present project.

## References

[1]Deiwert, G. S., "Numerical Simulation of High Reynolds Number Transonic Flow," *AIAA Journal*, Vol. 13, Oct. 1975, pp. 1354-1359.

[2]Steger, J. L., "Implicit Finite-Difference Simulation of Flow about Arbitrary Two-Dimensional Geometries," *AIAA Journal*, Vol. 16, July 1978, pp. 679-686.

[3]Mahgoub, H.E.H. and Bradshaw, P., "Calculation of Turbulent-Inviscid Flow Interaction with Large Normal Pressure Gradients," *AIAA Journal*, Vol. 17, Oct. 1979, pp. 1025-1029.

[4]Bauer, F., Garabedian, P. R., Korn, D. G., and Jameson, A., *Lecture Notes in Economics and Mathematical Systems*, No. 108, Springer-Verlag, Berlin, 1975.

[5]Bavitz, P. C., "An Analysis Method for Two-Dimensional Transonic Viscous Flows," NASA TND-7718, 1975.

[6]Jameson, A., "Numerical Computation of Transonic Flows with Shock Waves," *Symposium Transsonicum*, Vol. II, 1975, p. 384.

[7]Bradshaw, P., Mizner, G. A., and Unsworth, K., "Calculation of Compressible Turbulent Boundary Layers on Straight Tapered Swept Wings," *AIAA Journal*, Vol. 14, March 1976, pp. 399-400.

[8]Curle, N., *The Laminar Boundary Layer Equations*, Oxford University Press, Oxford, England, 1962.

[9]Bradshaw, P., "Compressible Turbulent Shear Layers," *Annual Review of Fluid Mechanics*, Vol. 9, 1977, pp. 35-54.

[10]Bradshaw, P., Dean, R. B., and McEligot, D. M., "Calculation of Interacting Turbulent Shear Layers: Duct Flows," *ASME Journal of Fluids Engineering*, Vol. 95, June 1973, pp. 214-219.

[11]Davis, R. T. and Rubin, S. G., "Non-Navier-Stokes Viscous Flow Computations," *Computers and Fluids*, Vol. 8, No. 1, 1980, pp. 101-131.

[12]Johnson, D. A. and Bachalo, W. D., "Transonic Flow about a Two-Dimensional Airfoil—Inviscid and Turbulent Flow Properties," AIAA Paper 78-1117, 1978.

[13]Gregory, N. and Wilby, P. G., "NPL 9615 and NACA 0012—A Comparison of Aerodynamic Data," ARC CP 1261, 1973.

[14]Collyer, M. R. and Lock, R. C., "Improvements to the Viscous Garabedian and Korn Method for Calculating Transonic Flow Past an Aerofoil," RAE TR 78039, 1978.

[15]Le Balleur, J. C., "Strong Matching Methods for Computing Transonic Viscous Flows Including Wakes and Separations. Lifting Aerofoils," *La Recherche Aerospatiale*, No. 3, 1981, pp. 1-19.